

Supplemental information

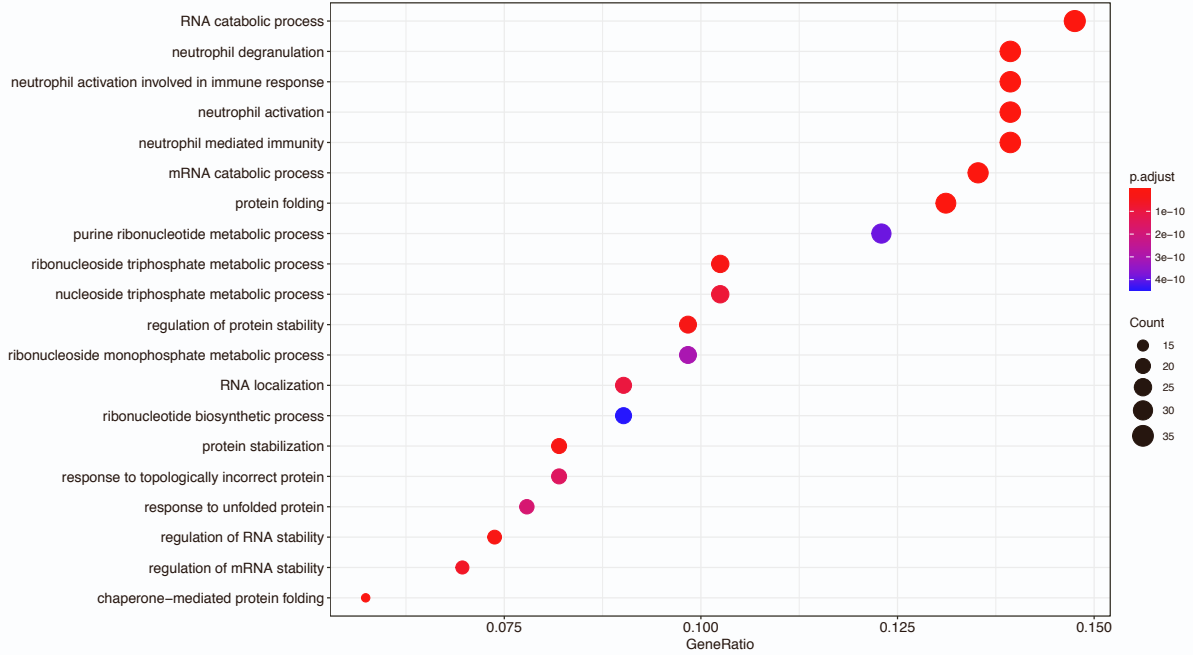
**SARS-CoV-2 nucleocapsid protein binds host
mRNAs and attenuates stress granules to
impair host stress response**

Syed Nabeel-Shah, Hyunmin Lee, Nujhat Ahmed, Giovanni L. Burke, Shaghayegh Farhangmehr, Kanwal Ashraf, Shuye Pu, Ulrich Braunschweig, Guoqing Zhong, Hong Wei, Hua Tang, Jianyi Yang, Edyta Marcon, Benjamin J. Blencowe, Zhaolei Zhang, and Jack F. Greenblatt

Figure S1

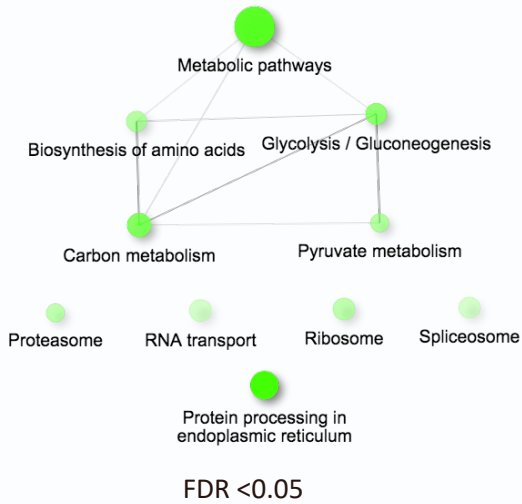
A

Biological processes enrichment



B

KEGG pathway enrichment



C

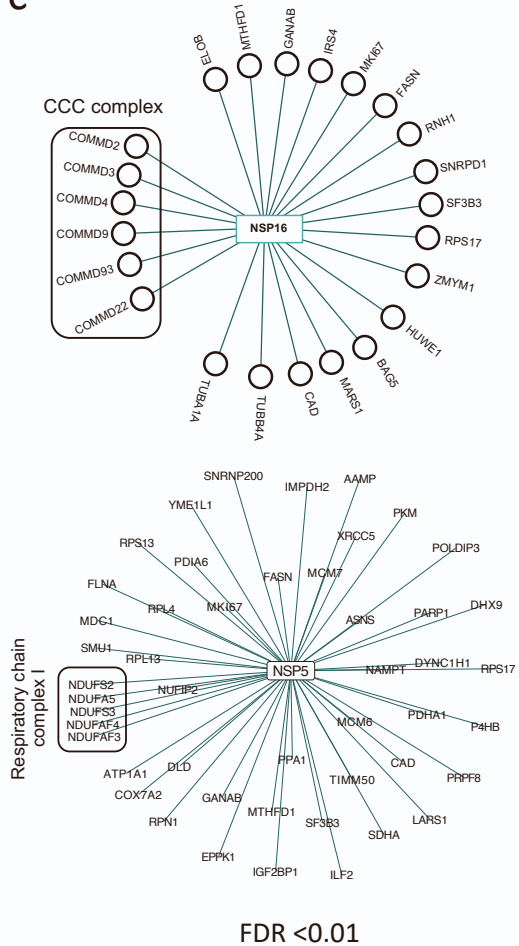


Figure S1: SARS-COV-2 protein interactions, related to Figure 1. A: GO enrichment analysis related to biological processes using cellular proteins identified as high confidence ($FDR \leq 1\%$) interaction partners for 27 SARS-CoV-2 proteins. **B:** KEGG pathway enrichment analysis using cellular proteins identified as high confidence ($FDR \leq 1\%$) interaction partners for the SARS-CoV-2 proteins. Darker nodes are more significantly enriched gene sets. Bigger nodes represent larger gene sets. Edge thickness represents overlap of genes. **C:** Network illustration of protein-protein interactions for selected SARS-CoV-2 bait proteins. Co-purifying subunits that belong to a specific protein-complex are grouped together.

Figure S2

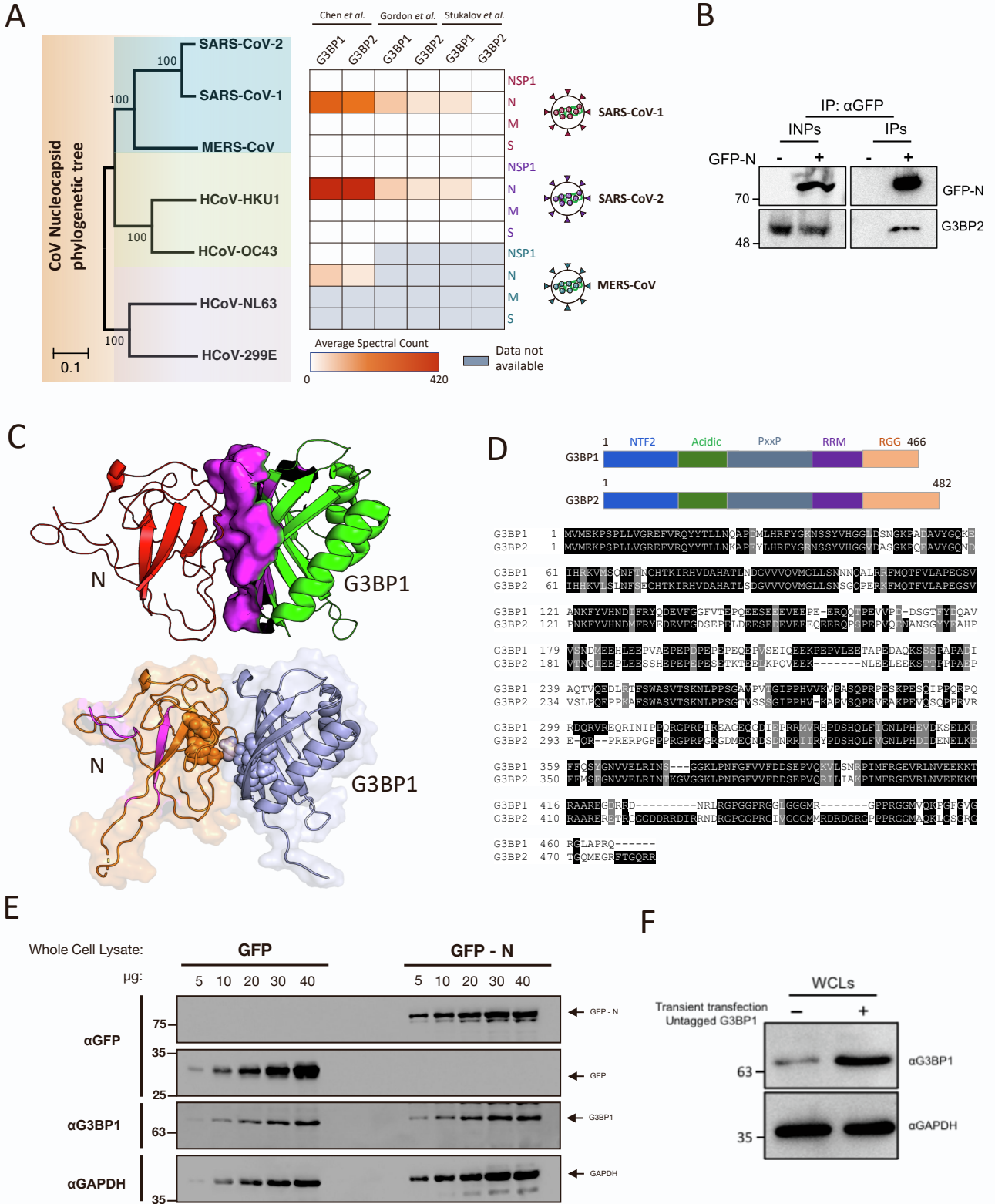


Figure S2: N specifically interacts with G3BP1 and G3BP2, related to Figures 1 and 2. **A:** Left, Protein phylogeny of N across indicated coronaviruses. Different clusters are highlighted in colors. Tree topology represents the Neighbour Joining (NJ) estimations. Confidence values are indicated based on 1,000 bootstrap replicas. The scale bar indicates the number of substitutions per site. Right, Heatmap illustration of SARS-CoV-2 proteins' interaction with stress granule proteins G3BP1 and G3BP2 across three different studies as indicated; (Gordon et al. 2020 [PMID: 33060197]; Stukalov et al. 2021 [PMID: 33845483]; Chen et al. 2021 [PMID: 34232536]). **B:** Interaction of SARS-CoV-2 N protein with G3BP2 detected by co-immunoprecipitation experiments. IPs were performed with GFP antibody using whole cell lysates prepared from control HEK293 cells or cells expressing GFP-N. Cell lysates were treated with nuclease prior to IPs. Blots were probed with the indicated antibodies. INPs and IPs had different exposure time. **C: Top:** Cartoon illustration of protein docking studies. The complex structure model between G3BP1 (4FCJ_A, green) and N protein (6M3M_B, red) is shown. The interface areas are shown as a purple surface. A residue is defined as an interface residue if it is within 6 Å of its binding partner. The interface area of G3BP1-N was 780.73 Å². The interface energy of the final model was -5.46, which indicates a reliable model according to the Rosetta document. **Bottom:** Alternative view of the complex structure model between G3BP1 (light blue cartoon) and the N protein (orange cartoon) is shown. The orange spheres and the light blue spheres are the predicted interface residues for N and G3BP1, respectively. The reported theoretical RNA-binding residues [PMID: 33264373] on N are highlighted in magenta. **D:** Top: Domain architecture of G3BP1 and G3BP2 proteins. Bottom: Multiple sequence alignment analysis using G3BP1 and G3BP2 protein sequences. Highly conserved residues are shaded in black. **E:** Western blotting analysis using whole cell extracts prepared from either GFP- or GFP-N-expressing cells. Blots were probed with indicated antibodies. **F:** Western blotting analysis using whole cell extracts prepared from cells transiently transfected with either G3BP1 or empty vector. Blots were probed with indicated antibodies.

Figure S3

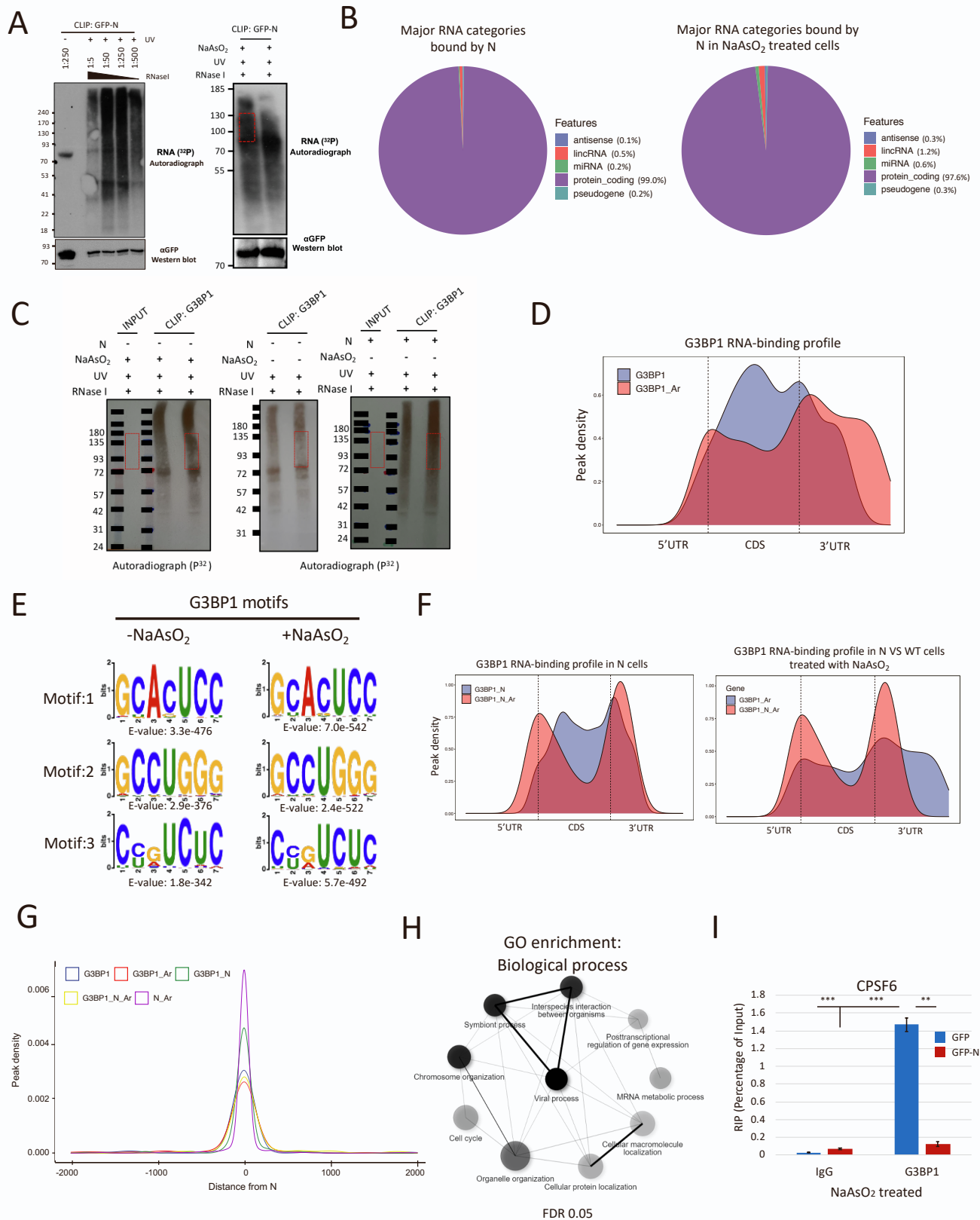
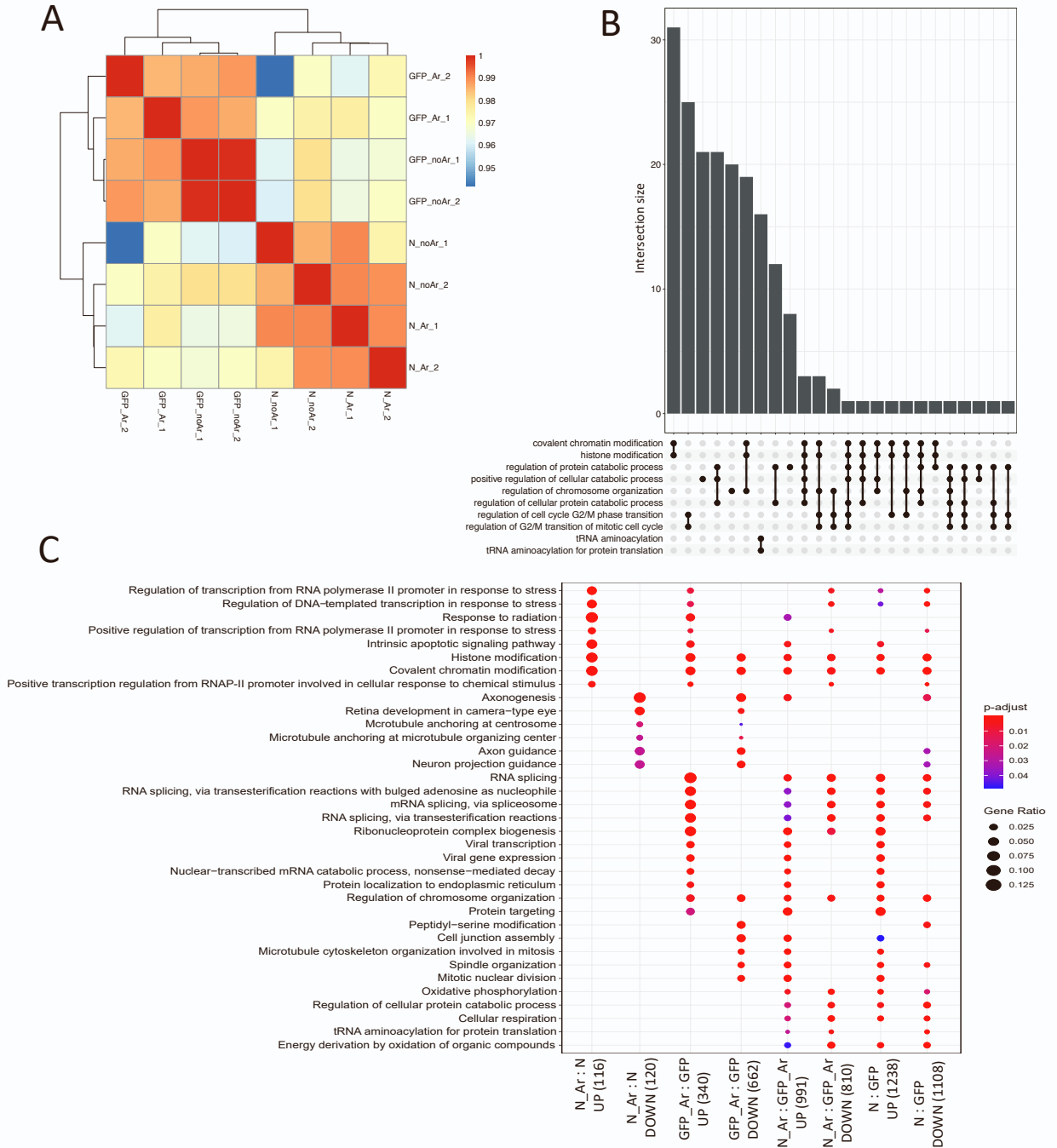


Figure S3: iCLIP analysis of N and G3BP1, related to Figures 3 and 4. A: Left, Autoradiographs of immunopurified ³²P-labeled N-RNA complexes after partial RNase I digestion at various dilutions. N-expressing HEK293 cells were UV-crosslinked and GFP-N was immunoprecipitated using anti-GFP antibody. Purified RNA-protein complexes were resolved on 4-12% Bis-Tris gels after radiolabeling the RNA and transferred to nitrocellulose membranes. Band in non-UV lane indicates radiolabeled N. Right, NaAsO₂-treated N-expressing HEK293 cells were used for CLIP-autoradiography. Red box indicates the region of membrane used to extract RNA **B:** Pie chart representing the distribution of N iCLIP peaks across various RNA categories in non-NaAsO₂- and NaAsO₂-treated cells. Legends are provided. **C:** Autoradiographs of immunopurified ³²P-labeled G3BP1-RNA complexes after partial RNase I digestion. 2% input samples were loaded in parallel to CLIP samples. CLIP was performed using anti-G3BP1 antibody. Red boxes indicate the regions of membrane used to extract RNA. **D:** Standardized metaplot profile showing the normalized peak density of G3BP1 iCLIP in non-NaAsO₂- and NaAsO₂-treated wildtype cells. CDS represents the coding sequence. **E:** Enriched sequence motifs found in G3BP1 iCLIP-seq peaks. E-value represents the significance of the motif against randomly assorted control sequences. **F:** Left: Standardized metaplot profile showing the normalized peak density of G3BP1 iCLIP in non-NaAsO₂- and NaAsO₂-treated N-expressing cells. Right: Standardized metaplot profile showing the normalized peak density of G3BP1 iCLIP in NaAsO₂-treated N-expressing and wildtype cells. CDS represents the coding sequence. **G:** Average iCLIP peak density of G3BP1 around N-binding sites. iCLIP-seq samples across different conditions are color coded and legend is provided. **H:** GO enrichment analysis related to biological processes using N-specific G3BP1 target genes (Q≤0.05). Darker nodes are more significantly enriched gene sets. Bigger nodes represent larger gene sets. Edge thickness represents overlap of genes. **I:** Bar graph representation of G3BP1 RIP-qPCR experiments in NaAsO₂-treated cells expressing either GFP-N or GFP showing the G3BP1 RNA-binding to *CPSF6* transcript. The experiments were performed in biological triplicates, and p-values were calculated using the student's t-test (**p≤0.01, ***p≤0.001). Error bars represent standard error of mean (SEM).

Figure S4



Supplementary Figure 4: RNA-seq analysis of N-expressing cells, related to Figure 5.

A: Heatmap illustration of correlation between RNA-seq biological replicates. Pearson correlation of co-efficient values for the heatmap are shown on the right. **B:** GO enrichment analysis using genes that were significantly downregulated in cells expressing GFP-N in comparison to cells expressing GFP. Only the top 10 most significant terms related to biological processes are shown ($Q \leq 0.05$). **C:** GO enrichment analysis using genes that were significantly differentially expressed across the indicated comparisons. p-values and gene counts for each GO term are provided.

Figure S5

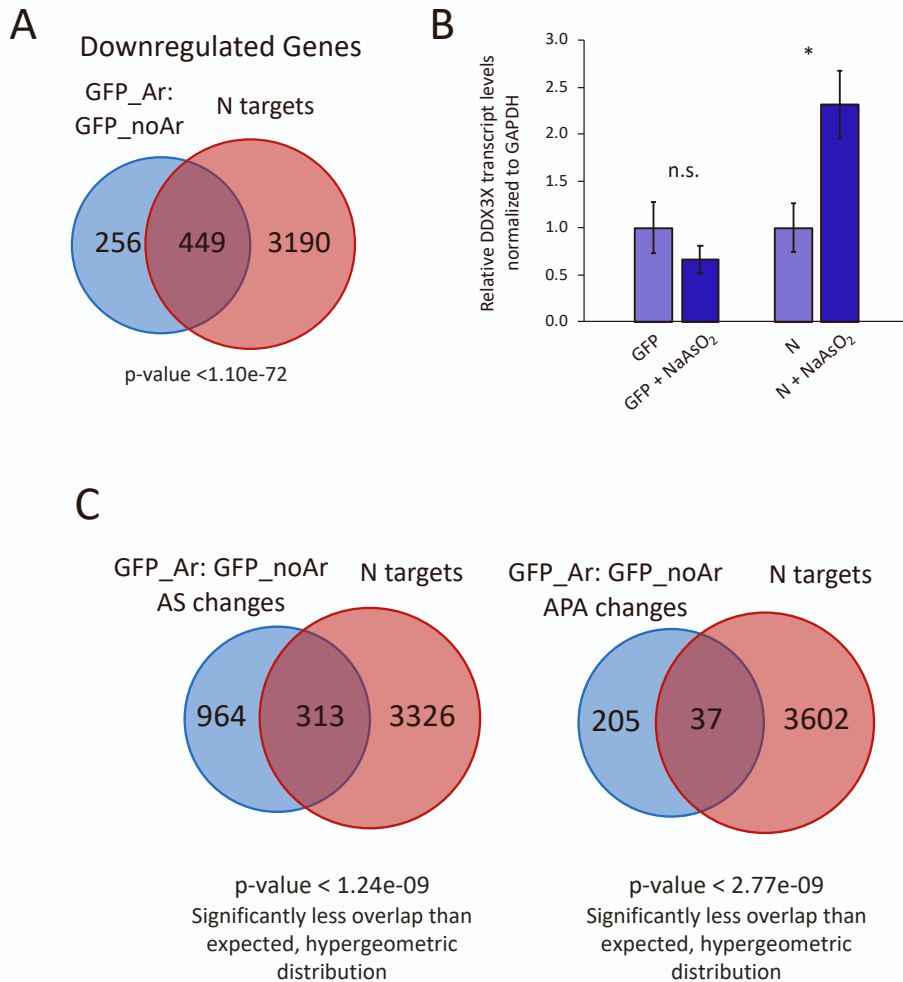


Figure S5: N reverses posttranscriptional changes induced in response to stress, related to Figure 6. **A:** Venn diagram showing the overlap of stress induced differential genes in wildtype GFP-expressing cells with those identified as N targets through iCLIP-seq. P-values were calculated using hypergeometric test. **B:** Bar graphs representing RT-qPCR results to examine the differential expression of selected targets in NaAsO₂-treated N-expressing and wildtype cells. The experiments were performed in biological triplicates, and p-value were calculated using the student's t-test (**p≤0.001, *p≤0.01, *p≤0.05, n.s.: non-significant). Error bars represent SEM. **C:** Venn diagram showing the overlap of stress induced AS (left) and APA (right) changing genes with those identified as N targets. P-values indicate the significant underrepresentation of AS and APA genes in N targets (hypergeometric distribution).

Figure S6

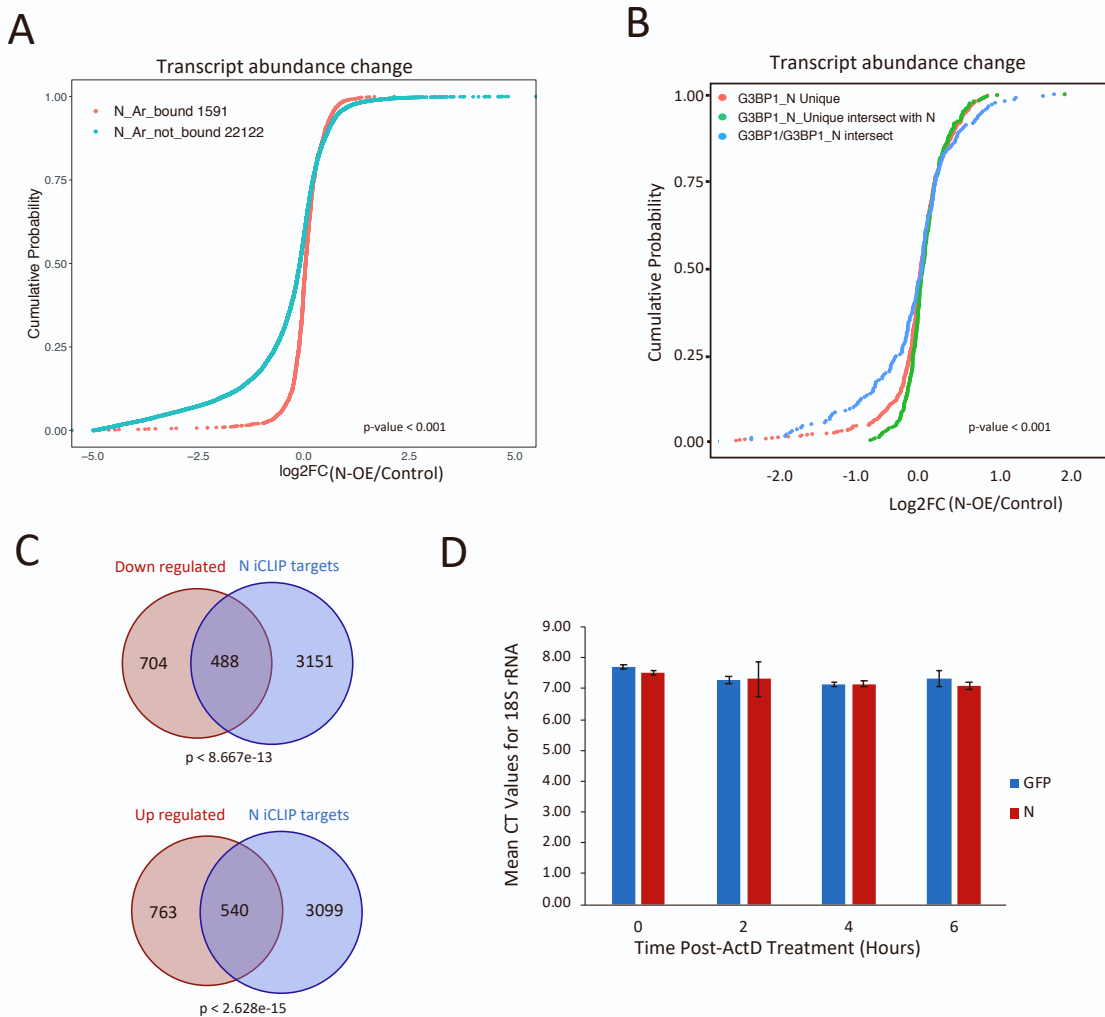


Figure S6: N modulates the stability of target mRNAs, related to Figure 6. A: Cumulative distribution analysis in abundance N iCLIP target mRNAs after N expression in NaAsO₂-treated HEK293 cells. P-value < 0.001 (Kruskal–Wallis test). **B:** Cumulative distribution analysis in abundance of G3BP1 target mRNAs after N overexpression in HEK293 cells. G3BP1 targets were identified by iCLIP-seq in N-expressing cells. Note: ‘G3BP1_N Unique’ represent those targets that were bound by G3BP1 only in N-expressing cells; ‘G3BP1_N_Unique intersect with N’ targets were obtained by overlapping ‘G3BP1_N Unique’ with N bound transcripts as defined by iCLIP-seq of N; ‘G3BP1/G3BP1_N intersect’ represent the common targets of G3BP1 in wildtype and N-expressing cells. Legend is provided. P-value < 0.001 (Kruskal–Wallis test). **C:** Venn diagram showing the overlap of differential genes in N-expressing cells with those identified as N targets through iCLIP-seq. P-values were calculated using hypergeometric test. **D:** Bar graph showing the RT-qPCR mean CT values for 18S rRNA transcripts across indicated time points after Actinomycin D treatment. Error bars represent standard error of mean (n=3).

Figure S7

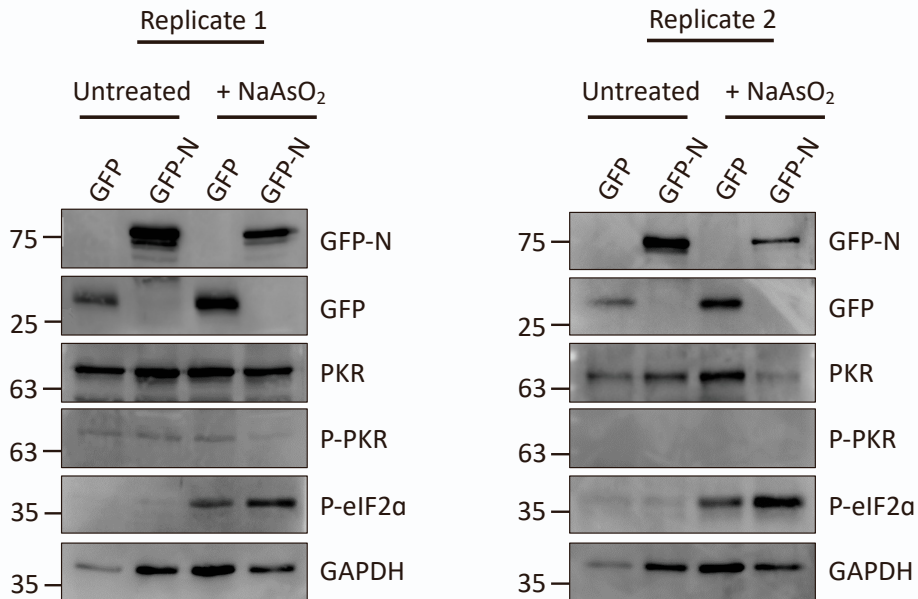


Figure S7: Effect of N on phosphorylation levels of PKR and eIF2α in non-NaAsO₂- and NaAsO₂-treated cells. Related to Figure 2. Western blotting analysis using whole cell extracts prepared from either GFP- or GFP-N-expressing non-NaAsO₂- and NaAsO₂-treated cells. Blots were probed with the indicated antibodies.